Clinical validation of the 3-dimensional double-echo steady-state with water excitation sequence of MR neurography for preoperative facial and lingual nerve identification

Dohyun Kwon(iD)[1,2], Chena Lee(iD)[3], YeonSu Chae(iD)[1], Ik Jae Kwon(iD)[1], Soung Min Kim(iD)[1], Jong-Ho Lee(iD)[1,*]

[1]Department of Oral and Maxillofacial Surgery, School of Dentistry, Seoul National University, Seoul, Korea
[2]Department of Oral and Maxillofacial Surgery, Samsung Medical Center, Seoul, Korea
[3]Department. of Oral and Maxillofacial Radiology, College of Dentistry, Yonsei University, Seoul, Korea

ABSTRACT

Purpose: This study aimed to evaluate the clinical usefulness of magnetic resonance (MR) neurography using the 3-dimensional double-echo steady-state with water excitation (3D-DESS-WE) sequence for the preoperative delineation of the facial and lingual nerves.
Materials and Methods: Patients underwent MR neurography for a tumor in the parotid gland area or lingual neuropathy from January 2020 to December 2021 were reviewed. Preoperative MR neurography using the 3D-DESS-WE sequence was evaluated. The visibility of the facial nerve and lingual nerve was scored on a 5-point scale, with poor visibility as 1 point and excellent as 5 points. The facial nerve course relative to the tumor was identified as superficial, deep, or encased. This was compared to the actual nerve course identified during surgery. The operative findings in lingual nerve surgery were also described.
Results: Ten patients with parotid tumors and 3 patients with lingual neuropathy were included. Among 10 parotid tumor patients, 8 were diagnosed with benign tumors and 2 with malignant tumors. The median facial nerve visibility score was 4.5 points. The distribution of scores was as follows: 5 points in 5 cases, 4 points in 1 case, 3 points in 2 cases, and 2 points in 2 cases. The lingual nerve continuity score in the affected area was lower than in the unaffected area in all 3 patients. The average visibility score of the lingual nerve was 2.67 on the affected side and 4 on the unaffected side.
Conclusion: This study confirmed that the preoperative localization of the facial and lingual nerves using MR neurography with the 3D-DESS-WE sequence was feasible and contributed to surgical planning for the parotid area and lingual nerve. *(Imaging Sci Dent 2022; 52: 259-66)*

KEY WORDS: Magnetic Resonance Imaging; Facial Nerve; Lingual Nerve Injuries; Parotid Neoplasms

Introduction

Nerve identification is essential for planning dental surgery involving tooth extraction or mass excision, especially in the parotid gland region. During the operation, nerve branches are difficult to visualize, and a preoperative delineation is essential for surgeons.

In particular, the identification of the facial nerve is crucial for the success of surgery, because postoperative facial nerve palsy after parotidectomy occurs in as many as 3%-4% of patients.[1,2] Conventional T1-weighted imaging (T1-WI) is a method used to visualize the facial nerve depending on the fatty tissue of the parotid gland. However, the boundary of the facial nerve is often blurred and difficult to detect on T1-WI.[3-5] Many reports have investigated ways of identifying the facial nerve in the parotid gland, but many of these methods were indirect.[6,7] Lingual nerve damage may manifest during third molar extraction or inferior alveolar nerve block. Although lingual nerve

damage occurs infrequently, patients with lingual nerve damage report substantial discomfort and neuropathic pain. However, it is challenging for clinicians to evaluate the extent of the damage because it is not easy to directly visualize the damage with conventional radiography.

Magnetic resonance (MR) imaging is a non-invasive modality with excellent soft tissue contrast. In addition, the recent development of the fast imaging technique has made it possible to obtain multi-directional views using image reconstruction.[8] Advances in MR neurography have enabled the direct visualization of peripheral nerves. Various MR neurography sequences have been developed, and it is important to select a proper imaging protocol according to the location of the peripheral nerve or the cause of the nerve pathology.

The 3-dimensional double-echo steady-state with water excitation (3D-DESS-WE) sequence was initially used for imaging of articular cartilage in the orthopedic field.[9,10] This sequence displays water as a highly intense signal, while it suppresses the signal from blood flow. The 3D-DESS-WE sequence has been introduced to visualize the intra-parotid facial nerve, and several studies have evaluated the efficacy of the sequence for identifying the extracranial branch of the cranial nerve.[11-13] In the 3D-DESS-WE sequence, a nerve is shown with high signal intensity resulting from its myelin layer through the water excitation and fat-suppression technique.[11]

Thus, this study aimed to investigate the feasibility and usefulness of MR neurography using the 3D-DESS-WE sequence for the preoperative identification of the nerve course. In particular, the accuracy of the localization of the facial nerve was evaluated since its relative location to the tumor is crucial for parotid gland surgery. For patients with lingual neuropathy, the continuity of the lingual nerve was investigated because information related to nerve continuity is important in deciding whether to perform surgical treatment. The MR neurography findings were verified by comparing them with actual surgical observations.

Materials and Methods

Patients who visited the Department of Oral and Maxillo-facial Surgery at Seoul National University Dental Hospital for a tumor in the parotid gland area or lingual neuropathy from January 2020 to December 2021 were included in this study. Patients' surgical records were thoroughly reviewed to investigate the operative procedure, pathology, and the surgical findings related to the nerve bundle pathway. This retrospective study was exempted from institutional review approval (IRB No. ERI21046).

MR neurography was acquired with either a 3.0-T Magnetom Skyra Fit 20-channel head coil (Siemens Healthcare, Erlangen, Germany) or a 3.0-T Pioneer 32-channel head coil (GE healthcare, Waukesha, WI, USA). For both units, MR neurography was obtained with the protocol based on the double-echo steady-state sequence. The sequence is most frequently referred to as 3D-DESS-WE, although major MRI manufacturers have also proposed multiple other acronyms have also been proposed, such as FAst Double Echo (FADE) or Multi-Echo iN Steady-state Acquisition (MENSA).[14] To reduce confusion, the term 3D-DESS-WE has been consistently used in this study. The detailed imaging parameters of the individual units are described in Table 1.

All images were evaluated by a board-certified oral and maxillofacial surgeon and a board-certified radiologist with more than 6 and 7 years of experience, respectively. They evaluated the images with sufficient discussion and consensus.

The overall nerve visibility on MR neurography was assessed, and the tumor-nerve relationship was evaluated. The overall nerve course from the stylomastoid foramen to

Table 1. Detailed scan parameters of magnetic resonance neurography

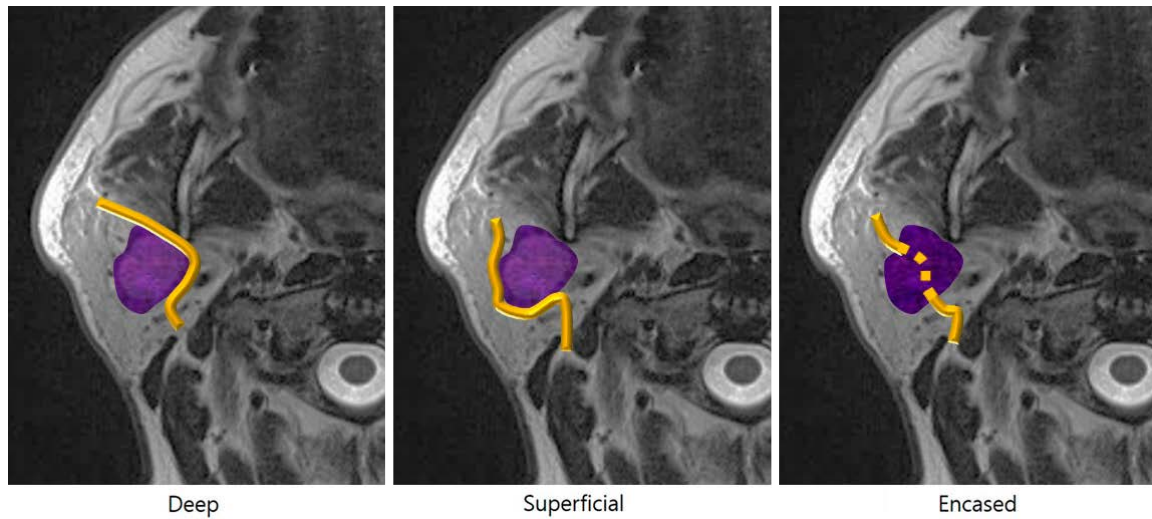| Equipment	3.0T Magnetom Skyra (Siemens)	3.0T Pioneer (GE)
Sequence	3-dimensional double echo steady-state with water excitation	Multi-echo in steady-state acquisition
TR (ms)	20.4	11
TE (ms)	10.3	4
FA (°)	30	30
FOV (mm)	200 × 200	200 × 200
Matrix	384 × 244	384 × 246
Voxel size (mm)	0.52 × 0.8 × 1.6	0.52 × 0.8 × 1.6
Acquisition time (min:sec)	4:56	5:19

Fig. 1. Schematic view of the tumor-to-facial nerve relationship.

the parotid space was evaluated in axial slice images with 1.6-mm thickness. The evaluation criteria followed those of a previous study:[15] 5 points: excellent nerve visualization with full diagnostic interpretability, 4 points: good nerve visibility with high confidence, 3 points: acceptable nerve visualization, 2 points: markedly reduced visibility and impaired diagnostic interpretability and 1 point: severely reduced visibility, allowing no diagnostic interpretability. The relative nerve location within the parotid gland was also determined. The axial, coronal, and sagittal section images were all reviewed by the same 2 observers mentioned above. Relative to the tumor, the facial nerve location was identified as superficial, deep, or encased (Fig. 1).

The overall lingual nerve visibility on MR neurography was assessed from the foramen ovale to the sublingual gland region. The evaluation was conducted with axial slice images of 1.6-mm thickness, and the same evaluation criteria as the facial nerve were applied. Additionally, discontinuity of the lingual nerve of both sides was assessed. When the clear nerve route was lost in at least 1 image slide, a discontinuity was considered to be present, whereas if there was no signal loss for the entire nerve course, a discontinuity was deemed to be absent.

Results

In total, 13 patients were included in the study, with a mean age of 46.8 years. There were 7 men and 6 women (Table 2). Ten patients underwent MR neurography for facial nerve evaluation and 3 patients for lingual nerve assessment.
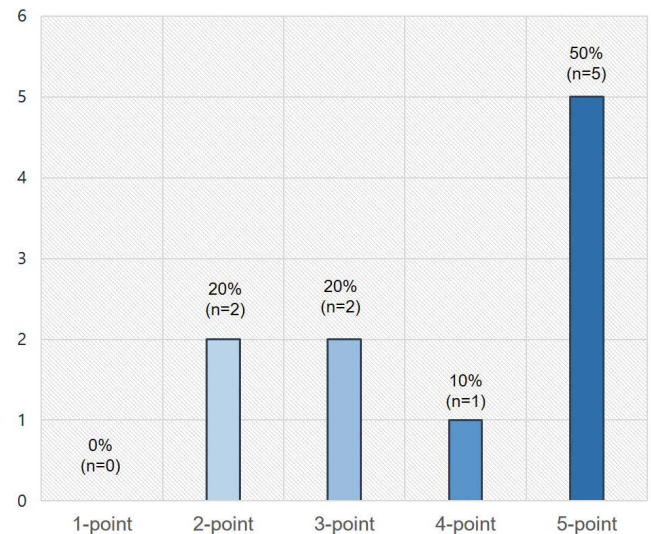

Fig. 2. Distribution of facial nerve visibility scores, with 5 points indicating excellent nerve visualization with full diagnostic inter-pre-tability; 4 points, good nerve visibility with high confidence; 3 points, acceptable nerve visualization; 2 points, markedly reduced visibility and impaired diagnostic interpretability; and 1 point, severely reduced visibility quality with no diagnostic interpretability.

For the 10 patients who underwent MR neurography for facial nerve, parotidectomy was performed and the final diagnoses were as follows: 7 pleomorphic adenomas, 1 carcinoma ex pleomorphic adenoma, 1 squamous cell carcinoma, and 1 case of nodular fasciitis. The median nerve visibility score was 4.5 points, with the following distribution: 5 points in 5 cases, 4 points in 1 case, 3 points in 2 cases, and 2 points in 2 cases (Fig. 2). Considering the actual nerve-tumor relationship, in 6 cases, the nerve was
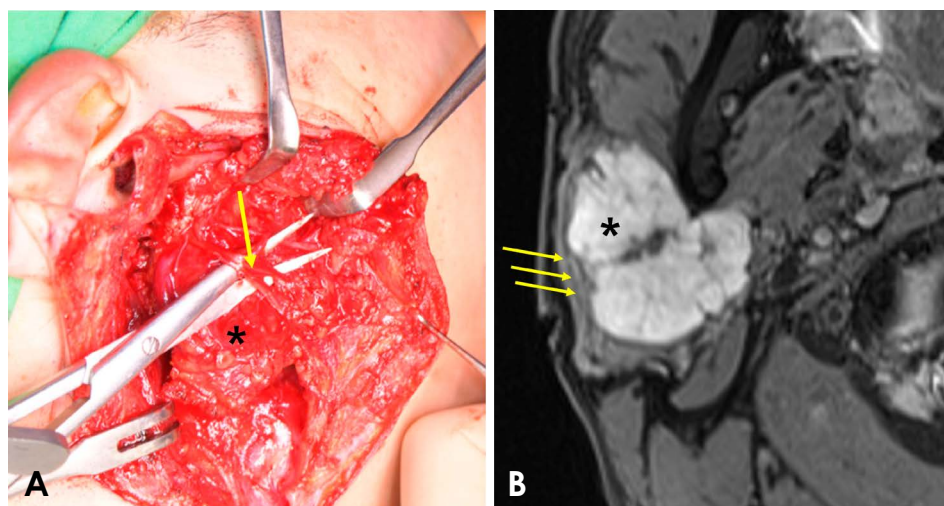
Fig. 3. A. The facial nerve is localized on the superficial aspect of the tumor. B. The axial view of magnetic resonance neurography reveals the nerve branch (arrow) located on the superficial side of the tumor (*). (*: tumor, arrow: nerve)

Table 2. Summary of patients in this study

Case	Age/Sex	Pathology	Location	Treatment
1	23/F	Traumatic neuropathy	Right lingual nerve	Observation
2	31/M	Pleomorphic adenoma	Right parotid gland	Parotidectomy, cervicofacial and auricular nerve repair
3	37/M	Pleomorphic adenoma	Right parotid gland	Superficial parotidectomy, greater auricular nerve repair
4	20/F	Traumatic neuropathy	Right lingual nerve	Lingual nerve decompression
5	33/F	Carcinoma ex pleomorphic adenoma	Left parotid gland	Parotidectomy, facial nerve repair
6	77/M	Squamous cell carcinoma	Left parotid gland	Superficial parotidectomy, sural nerve graft of facial nerve, buccal branch
7	65/F	Pleomorphic adenoma	Right parotid gland	Superficial parotidectomy
8	56/F	Nodular fasciitis	Left TMJ	Deep parotidectomy, TMJ reconstruction
9	40/M	Pleomorphic adenoma	Left parotid gland	Superficial parotidectomy
10	26/M	Traumatic neuropathy	Left lingual nerve	Neuroma excision, nerve decompression, sural nerve graft
11	28/M	Pleomorphic adenoma	Right parotid gland	Superficial parotidectomy
12	79/M	Pleomorphic adenoma	Right parotid gland	Parotidectomy
13	66/M	Pleomorphic adenoma	Left parotid gland	Parotidectomy

TMJ: temporomandibular joint

found deep to the tumor and 2 cases showed the nerve on the superficial aspect of the tumor (Figs. 3 and 4). In 2 cases, the nerve was encased within the tumor (Fig. 5, Table 3). The nerve localization on MR neurography was consistent with the surgical findings in 9 cases, whereas 1 case showed an inconsistency between the intraoperative findings and MR neurography; in this case, the nerve was found to be encased in the tumor during surgery, whereas it was not clearly defined around the tumor on MR neurography.

In the 3 patients with lingual neuropathy, the lingual nerve course on MR neurography was assessed (Figs. 6 and 7). Two patients were treated with surgery, and 1 of them had neuroma (Table 3). The median nerve visibility

Table 3. Tumor-nerve relationship based on intraoperative findings and magnetic resonance neurography

Case	Intraoperation	MR neurography
2	Superficial	Superficial
3	Deep	Deep
5	Encased	Encased
6*	Encased	Not determined
7	Superficial	Superficial
8	Deep	Deep
9	Deep	Deep
11	Deep	Deep
12	Deep	Deep
13	Deep	Deep

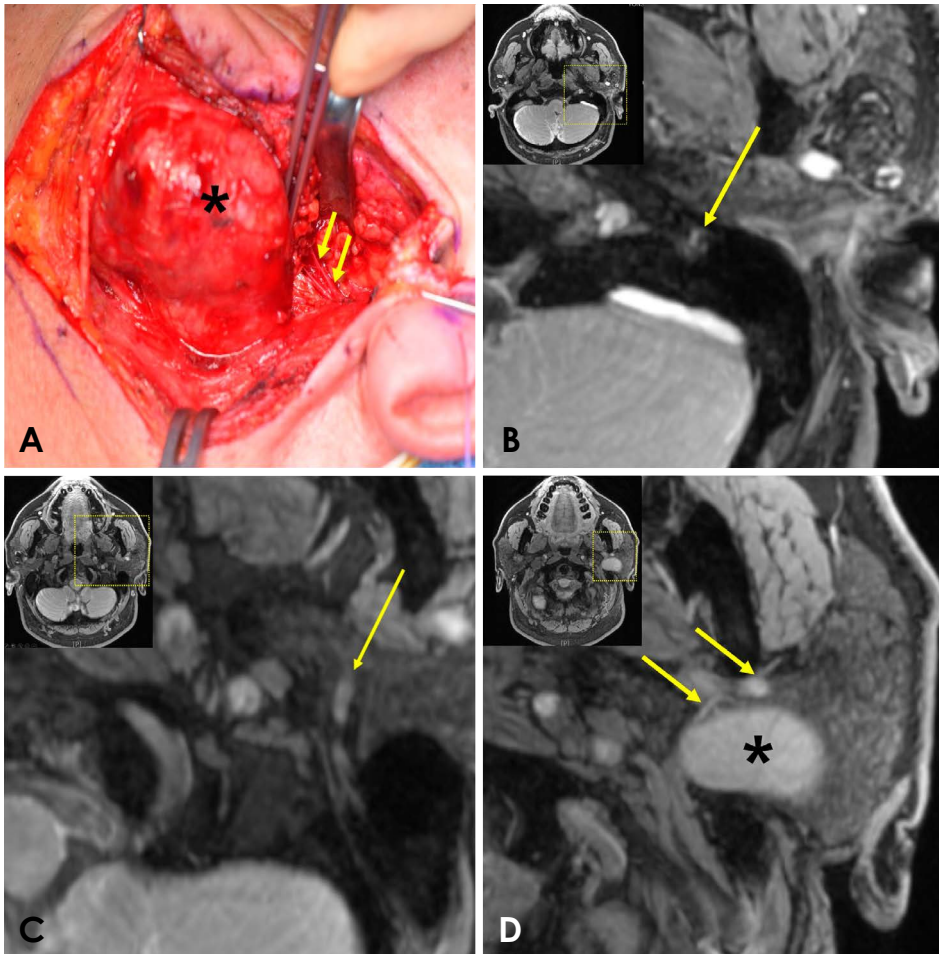*, inconsistency between surgical and imaging finding

Fig. 4. A. Intraoperative photograph presents the nerve deep to the tumor mass. B. In the axial view of magnetic resonance neurography, the facial nerve is near the stylomastoid foramen (arrow). C. Course of the facial nerve main trunk (arrow). D. The facial nerve closely contacts the tumor on the deep aspect. (*: tumor, arrow, nerve)
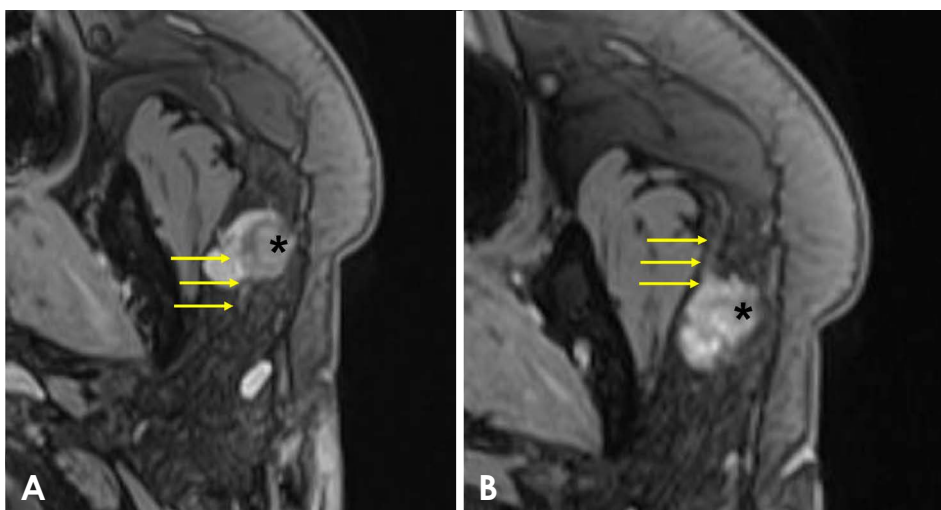

Fig. 5. A. In an axial view of magnetic resonance neurography, the buccal branch of the facial nerve is encased within the tumor. B. The buccal branch of the facial nerve exists within the tumor. (*, tumor; arrow, nerve)

score was 3.5 points. The score of the affected area was lower than that of the unaffected area for all patients (Table 4). No patients showed nerve discontinuity on MR neurography.

Discussion

Until recently, direct visualization of peripheral nerve branches was challenging. Hence, many studies made
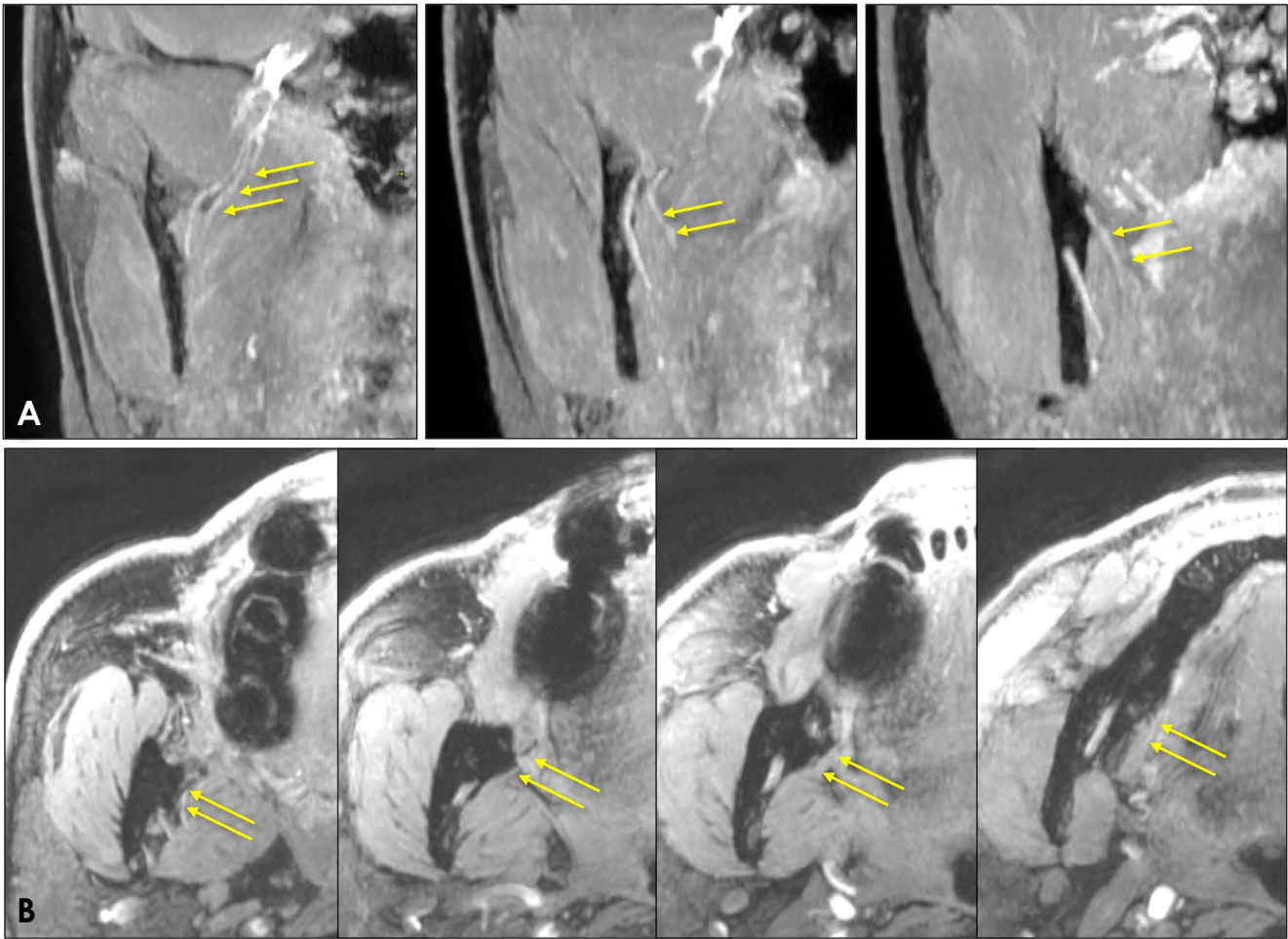
Fig. 6. A representative image of magnetic resonance neurography of the lingual nerve in this study. A. Coronal sectional view. B. Axial sectional view (arrow, lingual nerve).

Fig. 7. The lingual nerve is unclear, with haziness on the affected side (thick arrow), and is clearly shown on the unaffected side (arrow).

efforts to establish visualization methods for the facial nerve using MR imaging.[16] In the current study, the facial nerve within the parotid space was evaluated using a relatively recent imaging technique, 3D-DESS-WE MR neurography, and the imaging findings were quite consistent with the actual nerve course in most cases. Several recent studies have also reported that 3D-DESS-WE MR neurography showed an excellent ability to detect the main trunk, cervicofacial, and temporofacial divisions of the facial nerve.[7,13,17]

Clinical symptoms of lingual nerve damage vary from hypoesthesia to altered sensations and neuropathic pain, and lingual nerve damage often reduces affected individuals' quality of daily life.[18] For maxillofacial surgeons, it has generally been difficult to decide whether to perform surgical treatment in patients referred for lingual nerve injury.[19] This was because until recently, there has been no direct way to visualize the lingual nerve, and most clini-

Table 4. Visibility score and discontinuity evalaution of the lingual nerve

Case	Damaged nerve side	Treatment procedure	Visibility score		Discontinuity of the damaged nerve
			Unaffected side	Affected side	
1	Right	Observation	4	2	Absence
4	Right	Nerve decompression	4	3	Absence
10	Left	Neuroma excision, nerve decompression, sural nerve graft	4	3	Absence

cal decisions relied on the patient's subjective reports of symptoms and neurosensory testing. However, the diagnosis of lingual neuropathy using neurosensory testing has limitations.

In contrast, 3D-DESS-WE MR neurography allows direct visualization of the lingual nerve, which offers significant assistance in making clinical decisions. If the lingual nerve is cut or a neuroma forms due to iatrogenic damage by surgical instruments, surgery is often required. However, in cases of needle stick injury to the lingual nerve during block anesthesia, surgical treatment is unnecessary. Thus, it is particularly important to evaluate the continuity of the lingual nerve and the presence of neuroma formation. Tracing the lingual nerve through 3D-DESS-WE MR neurography, along with an in-depth consultation with the dentist who referred the patient, will be more helpful than previous methods for establishing treatment plans for patients with lingual nerve damage.

The 3D-DESS-WE sequence used in the present study was primarily used to evaluate degenerative joint changes in the orthopedic field.[6] This sequence displays fluid with an extremely bright signal, while showing bone as dark with high resolution.[20] This technique has recently been adopted in MR neurography due to its ability to show nerves with a bright signal due to the endoneurium fluid while suppressing the blood signal.[7,13,20] In addition, compared to conventional T1-WI imaging, which is acquired slice by slice, the 3D-DESS-WE sequence is obtained as a 3D volume image that can freely be reconstructed into a multi-dimensional view. This method is advantageous for observing peripheral nerves with a thin diameter and irregular course. 3D-DESS-WE MR neurography successfully detected the facial nerve accurately in most cases in the current study.

In this study, 40% of the cases showed the facial nerve as being superficial to the tumor or encased within it, while 60% showed the nerve on the deep aspect of the tumor. When the tumor is located superficially, postoperative facial palsy is less likely to occur. However, when

tumors located deeper than the facial nerve are difficult to remove due to the overlying facial nerve. It takes more time to dissect the facial nerve from the tumor. The facial nerve is sometimes intentionally cut and then directly repaired (cases 2 and 5), or a nerve graft (case 6) is performed using the sural nerve or other nerves. These procedures make parotid mass removal difficult and increase the total operating time. Thus, 3D-DESS-WE MR neurography is very helpful for surgeons to perform the operation more comfortably and confidently, enabling the overall operation time to be reduced. The limitations of this study are that the number of samples was relatively small, and as a retrospective study, images were acquired with equipment from 2 different companies.

Therefore, it is crucial to understand the relative location of the tumor to the facial nerve in the parotid gland before surgery. The 3D-DESS-WE sequence for MR neurography is useful for delineating the facial nerve correctly. Preoperative planning using MR neurography with the 3D-DESS-WE sequence can enable the surgeon to understand the spatial relationship of facial nerve with the tumor, which would lead to surgical success and a good prognosis. Furthermore, in patients with lingual neuropathy, this MR neurography technique helps clinicians make clinical decisions regarding whether to proceed with surgical treatment.

Conflicts of Interest: None

References

1. O'Brien CJ. Current management of benign parotid tumors - the role of limited superficial parotidectomy. Head Neck 2003; 25: 946-52.
2. Guntinas-Lichius O, Gabriel B, Klussmann JP. Risk of facial palsy and severe Frey's syndrome after conservative parotidectomy for benign disease: analysis of 610 operations. Acta Otolaryngol 2006; 126: 1104-9.
3. Dailiana T, Chakeres D, Schmalbrock P, Williams P, Aletras A. High-resolution MR of the intraparotid facial nerve and parotid duct. AJNR Am J Neuroradiol 1997; 18: 165-72.
4. Held P, Fellner C, Fellner F, Seitz J, Strutz J. MRI of inner ear

anatomy using 3D MP-RAGE and 3D CISS sequences. Br J Radiol 1997; 70: 465-72.

5. Takahashi N, Okamoto K, Ohkubo M, Kawana M. High-resolution magnetic resonance of the extracranial facial nerve and parotid duct: demonstration of the branches of the intraparotid facial nerve and its relation to parotid tumours by MRI with a surface coil. Clin Radiol 2005; 60: 349-54.

6. Ariyoshi Y, Shimahara M. Determining whether a parotid tumor is in the superficial or deep lobe using magnetic resonance imaging. J Oral Maxillofac Surg 1998; 56: 23-7.

7. Kim Y, Jeong HS, Kim HJ, Seong M, Kim Y, Kim ST. Three-dimensional double-echo steady-state with water excitation magnetic resonance imaging to localize the intraparotid facial nerve in patients with deep-seated parotid tumors. Neuroradiology 2021; 63: 731-9.

8. Chhabra A, Lee PP, Bizzell C, Soldatos T. 3 Tesla MR neurography - technique, interpretation, and pitfalls. Skeletal Radiol 2011; 40: 1249-60.

9. Sewerin P, Schleich C, Vordenbäumen S, Ostendorf B. Update on imaging in rheumatic diseases: cartilage. Clin Exp Rheumatol 2018; 36 Suppl 114: 139-44.

10. Hardy PA, Recht MP, Piraino D, Thomasson D. Optimization of a dual echo in the steady state (DESS) free-precession sequence for imaging cartilage. J Magn Reson Imaging 1996; 6: 329-35.

11. Qin Y, Zhang J, Li P, Wang Y. 3D double-echo steady-state with water excitation MR imaging of the intraparotid facial nerve at 1.5T: a pilot study. AJNR Am J Neuroradiol 2011; 32: 1167-72.

12. Fujii H., Fujita A., Yang A., Kanazawa H., Buch K., Sakai O, et al. Visualization of the peripheral branches of the mandibular division of the trigeminal nerve on 3D double-echo steady-state with water excitation sequence. AJNR Am J Neuroradiol 2015; 36: 1333-7.

13. Fujii H, Fujita A, Kanazawa H, Sung E, Sakai O, Sugimoto H. Localization of parotid gland tumors in relation to the intraparotid facial nerve on 3d double-echo steady-state with water excitation sequence. AJNR Am J Neuroradiol. 2019; 40: 1037-42.

14. Hargreaves BA. Rapid gradient-echo imaging. J Magn Reson Imaging 2012; 36: 1300-13.

15. Friedrich B, Wostrack M, Ringel F, Ryang YM, Förschler A, Waldt S, et al. Novel metal artifact reduction techniques with use of slice-encoding metal artifact correction and view-angle tilting MR imaging for improved visualization of brain tissue near intracranial aneurysm clips. Clin Neuroradiol 2016; 26: 31-7.

16. Teresi LM, Kolin E, Lufkin RB, Hanafee WN. MR imaging of the intraparotid facial nerve: normal anatomy and pathology. AJR Am J Roentgenol 1987; 148: 995-1000.

17. Burian E, Probst FA, Weidlich D, Cornelius CP, Maier L, Robl T, et al. MRI of the inferior alveolar nerve and lingual nerve - anatomical variation and morphometric benchmark values of nerve diameters in healthy subjects. Clin Oral Investig 2020; 24: 2625-34.

18. Agbaje JO, Van de Casteele E, Hiel M, Verbaanderd C, Lambrichts I, Politis C. Neuropathy of trigeminal nerve branches after oral and maxillofacial treatment. J Maxillofac Oral Surg 2016; 15: 321-7.

19. Rood JP. Lingual nerve damage. Br Dent J 1996; 181: 121.

20. Eladawi S, Balamoody S, Amerasekera S, Choudhary S. 3T MRI of wrist ligaments and TFCC using true plane oblique 3D T2 Dual Echo Steady State (DESS) - a study of diagnostic accuracy. Br J Radiol 2022; 95: 20210019.